

Supporting Information

A triphenylamine scaffold for fluorogenic sensing of noxious cyanide via ICT mechanism and its bioimaging application

Amitav Biswas,^[a] Rimi Mukherjee,^[b] Atanu Maji,^[a] Rahul Naskar,^[a] Krishnendu Aich,^[a] Nabendu Murmu^[b] and Tapan K. Mondal^{*[a]}

[a] Department of Chemistry, Jadavpur University, Kolkata- 700032, India.

[b] Department of Signal Transduction and Biogenic Amines (STBA), Chittaranjan National Cancer Institute, Kolkata- 700026, India.

CONTENTS

Fig. S1. ¹H NMR (400 MHz) spectrum of the probe (PBIA) in DMSO-d₆

Fig. S2. ¹³C NMR (100 MHz) spectrum of the probe (PBIA) in DMSO-d₆

Fig. S3. IR spectrum of PBIA

Fig. S4. HRMS spectrum of PBIA

Fig. S5: ¹H-¹H-2D COSY NMR spectrum of PBIA in DMSO-d₆

Fig. S6: ¹H-¹³C-2D HSQC NMR spectrum of PBIA in DMSO-d₆

Fig. S7. Jobs plot of PBIA for CN⁻

Fig. S8. Time dependent absorption spectra of PBIA towards CN⁻

Fig. S9. Determination of detection limit (LOD)

Fig. S10. Change in UV-Vis spectra of the probe (PBIA) (20 μM) in presence of 40 μM of various anions

Fig. S11. Change in Fluorescence spectra of the probe (PBIA) (20 μM) in presence of 40 μM of various anions

Fig. S12. pH study of PBIA for CN⁻ (Fluorescence spectra)

Fig. S13. pH study of PBIA for CN⁻ (Absorption spectra)

Fig. S14. Stern-Volmer plot for CN⁻

Fig. S15. Emission spectra of PBIA (20μM) with different water fraction(f_w)

Fig. S16. ¹H NMR of PBIA-CN⁻ adduct

Fig. S17. HRMS of PBIA-CN⁻ adduct

Fig. S18. Contour plots of some selected molecular orbitals of PBIA

Fig. S19. Contour plots of some selected molecular orbitals of PBIA-CN⁻

Fig. S20. MTT assay of PBIA on breast cancer cell lines (MDA-MB231)

Fig. S21: Fluorescence spectral titration of the probe solution PBIA (20 μM) with the addition of CN^- in drinking water.

Fig. S22: Fluorescence spectral titration of the probe solution PBIA (20 μM) with the addition of CN^- in tap water.

Fig. S23: Fluorescence spectral titration of the probe solution PBIA (20 μM) with the addition of CN^- in lake water.

Table S1. Vertical electronic transitions calculated by TDDFT/B3LYP/CPCM method for PBIA and PBIA- CN^- in DMSO.

Table S2: Fluorescence lifetime data

Table S3. Comparison table for PBIA with others previously reported receptors

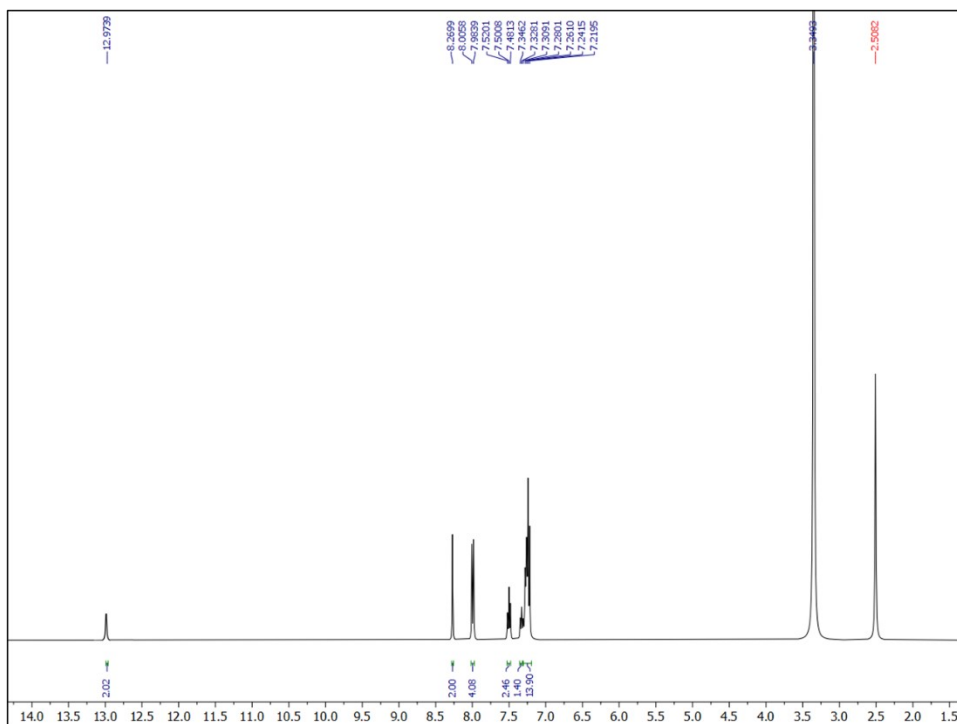


Fig. S1: ^1H NMR (400 MHz) spectrum of the probe (PBI A) in DMSO-d_6 .

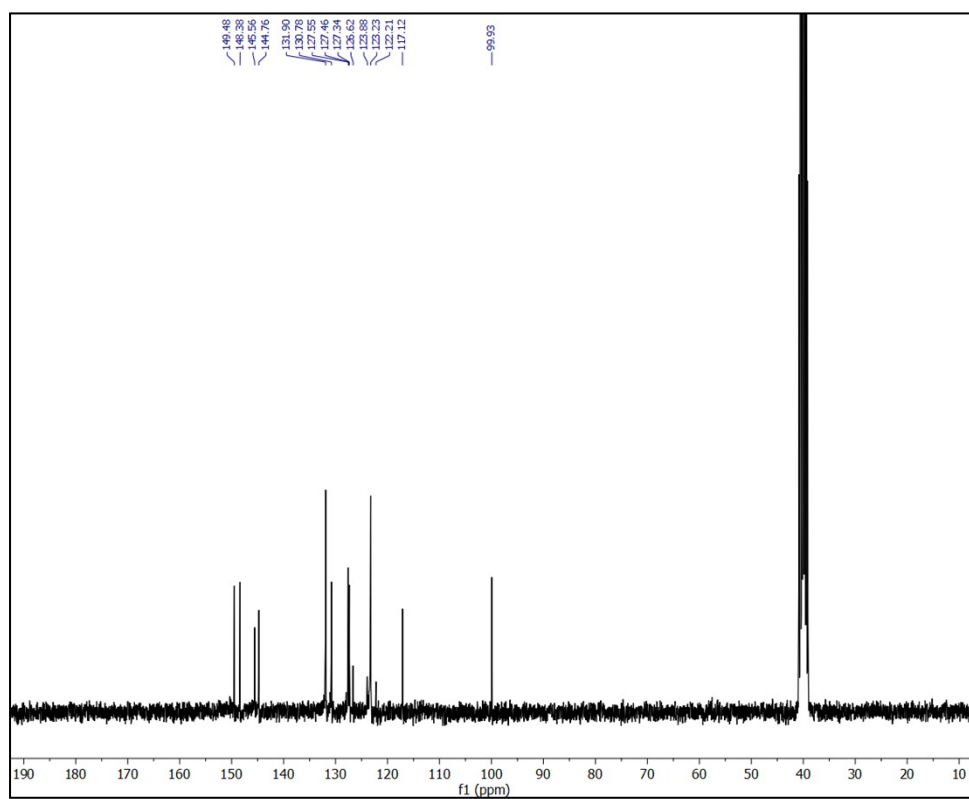


Fig. S2: ^{13}C NMR (100 MHz) spectrum of the probe (PBI A) in DMSO-d_6 .

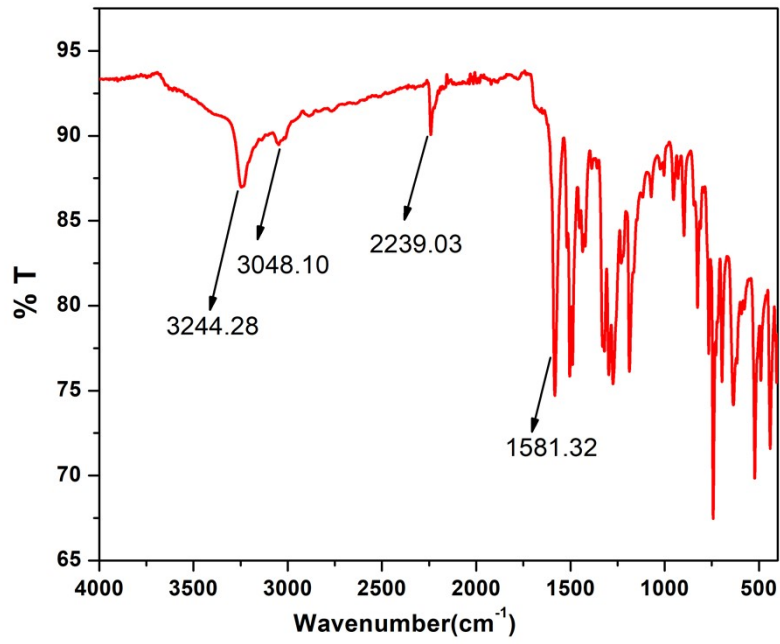


Fig. S3: IR Spectrum of PBIA.

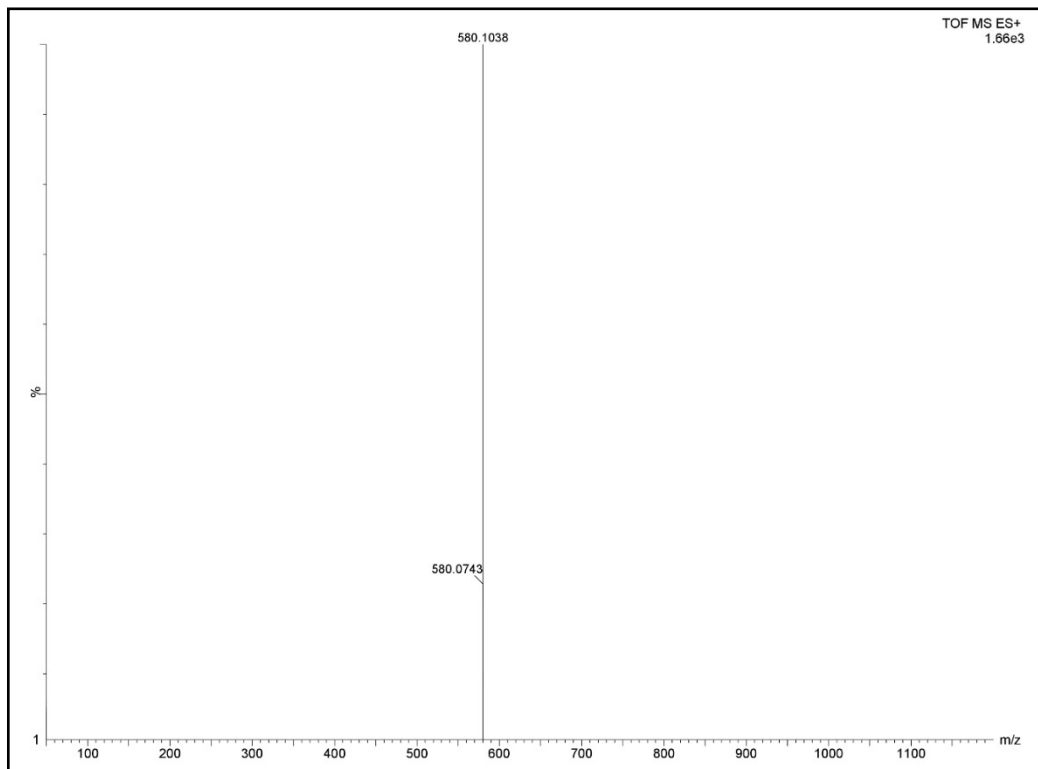


Fig. S4: HRMS of the probe (PBIA).

2D NMR study:

To validate the structural analysis further, we have done ^1H - ^1H 2D COSY NMR. Based on ^1H - ^1H 2D COSY correlation it was observed that the proton peak at 8.26 ppm correlates with the proton peak at 7.99 ppm, which proved that the vinylic proton (a) is correlating with the equivalent phenylic protons (b). Other correlations are also mentioned in the 2D homoneuclear correlation technique, which belongs to other phenylic aromatic proton interactions (Fig. S5).

Again to further confirm the peak position of vinylic proton, we have performed ^1H - ^{13}C 2D HSQC NMR. We observed that, among the four highly deshielded carbon atoms (position 1,7,10,17), only the carbon atom (7) at 144.8 ppm correlates with the vinylic proton, signal at 8.26 ppm (Fig. S6). Other correlations in ^1H - ^{13}C 2D HSQC NMR are associated with the carbon and protons of phenylic rings. So this 2D heteroneuclear correlation technique HSQC also resonates with the fact that 8.26 ppm peak belongs to vinylic proton.

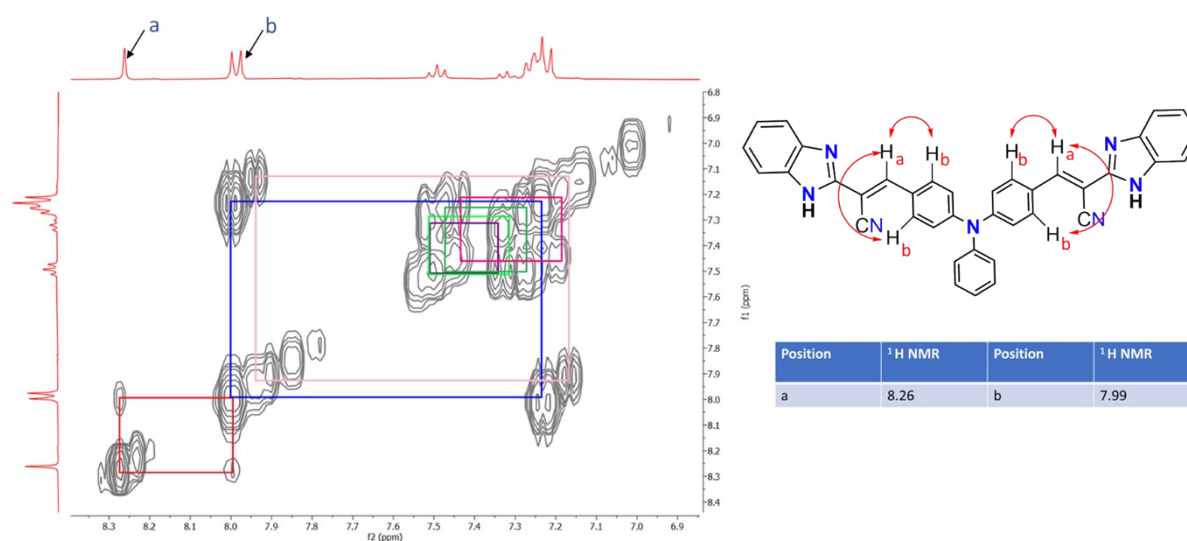


Fig. S5: ^1H - ^1H -2D COSY NMR spectrum of PBIA in DMSO-d_6 .

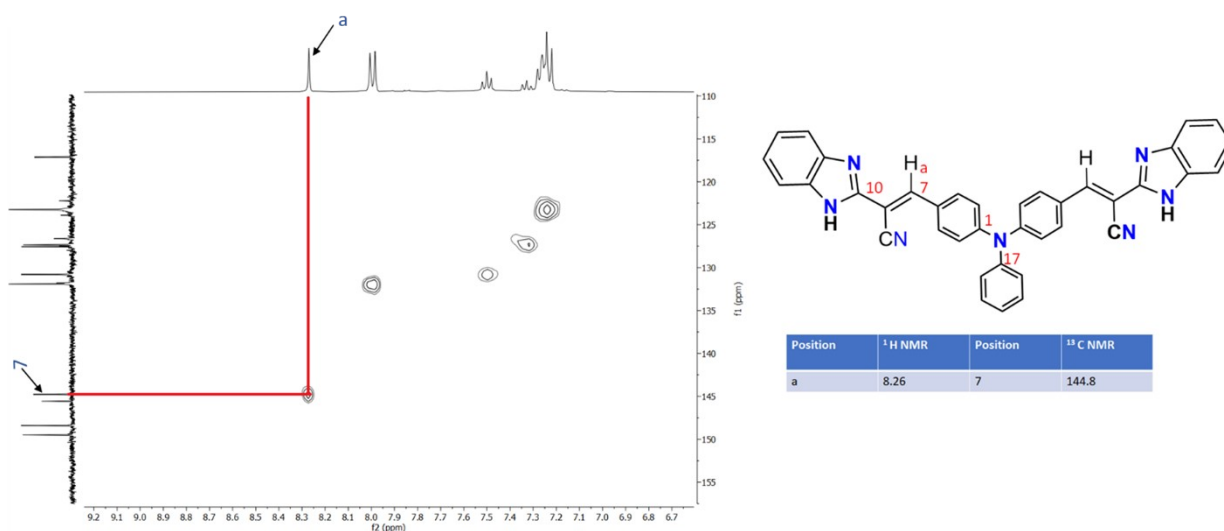


Fig. S6: ^1H - ^{13}C -2D HSQC NMR spectrum of PBIA in DMSO-d_6 .

Job's plot by absorbance method:

For Job's plot experiment, a series of solutions containing probe **PBIA** and CN^- were prepared in such a manner that the sum of the total anion and PBIA volume remained constant in DMSO medium. Then Job's plots was drawn by plotting A_{455} versus X_{CN^-} . (A_{455} = absorption spectrum at 455 nm for CN^- ion respectively and X_{CN^-} is the mole fraction of the CN^- solution).

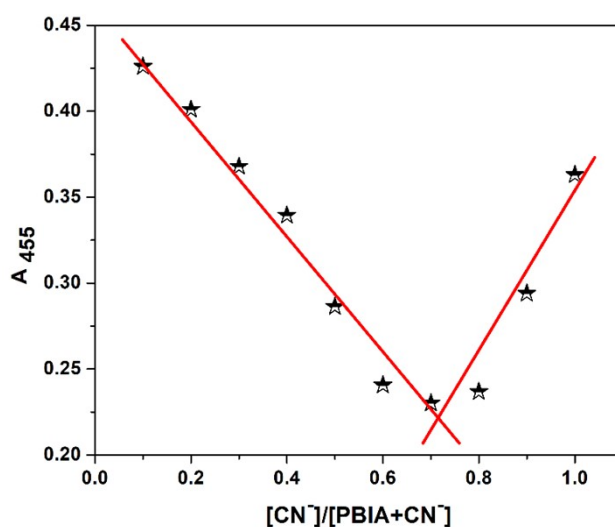


Fig. S7: Job's plot diagram of PBIA for CN^- .

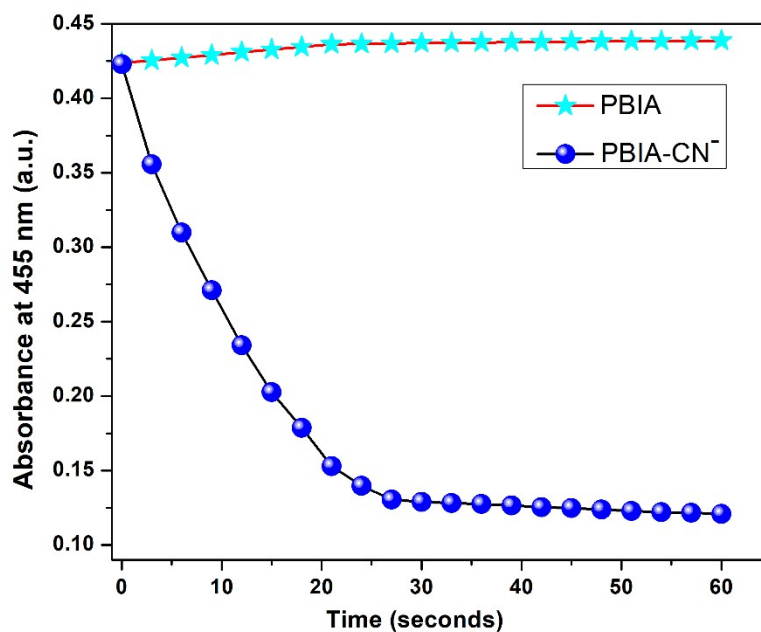


Fig. S8: The time-dependent absorption spectrum of PBIA towards CN⁻ in DMSO.

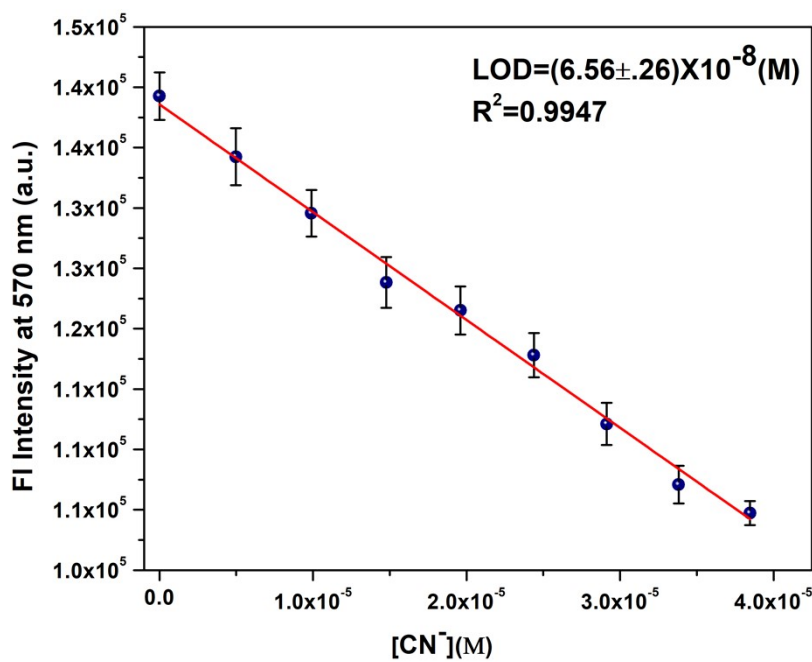


Fig. S9: Linear response curve of PBIA at 570 nm depending on the CN⁻ concentration.

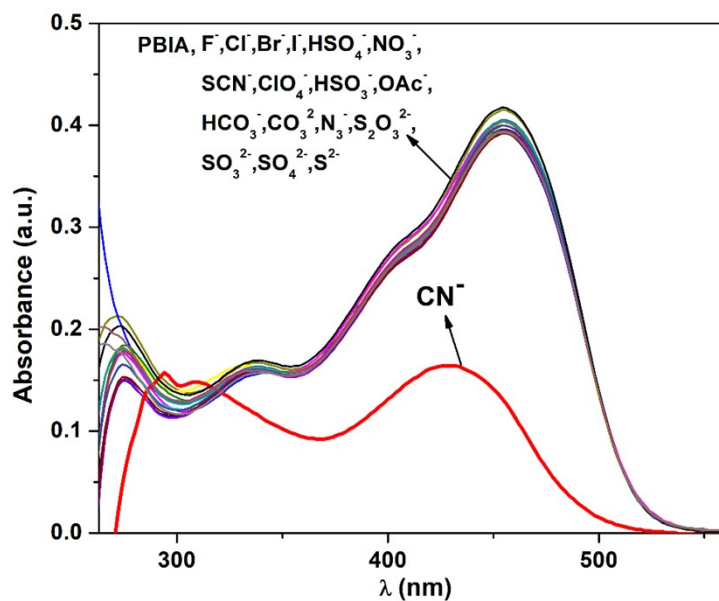


Fig. S10: Changes in UV-Vis spectra of PBIA (20 μM) upon addition of different anions, i.e. F^- , Cl^- , Br^- , I^- , HSO_4^- , NO_3^- , SCN^- , ClO_4^- , HSO_3^- , OAc^- , HCO_3^- , CO_3^{2-} , N_3^- , $\text{S}_2\text{O}_3^{2-}$, SO_3^{2-} , SO_4^{2-} , S^{2-} and CN^- (40 μM) in DMSO.

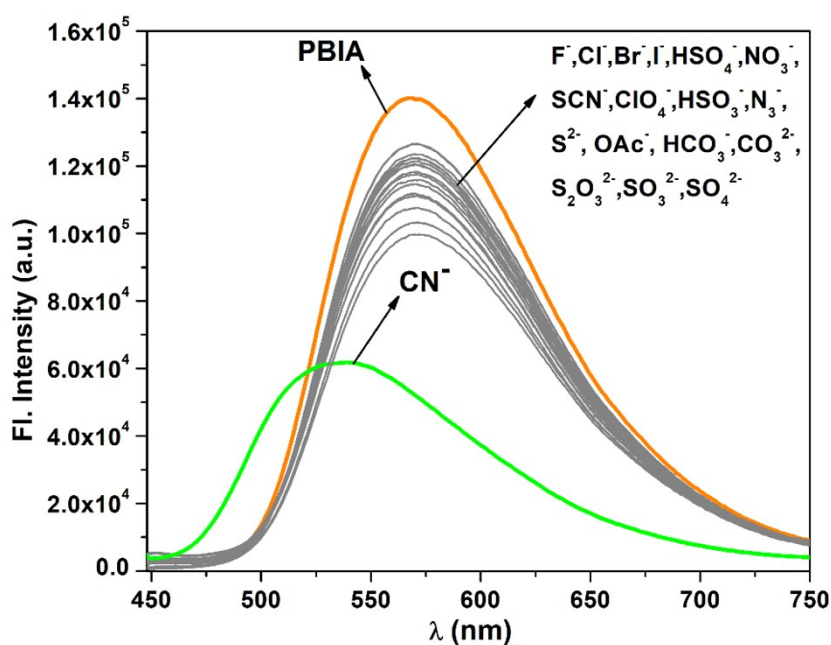


Fig. S11: Changes in emission spectra of PBIA (20 μM) upon addition of different anions, i.e. F^- , Cl^- , Br^- , I^- , HSO_4^- , NO_3^- , SCN^- , ClO_4^- , HSO_3^- , OAc^- , HCO_3^- , CO_3^{2-} , N_3^- , $\text{S}_2\text{O}_3^{2-}$, SO_3^{2-} , SO_4^{2-} , S^{2-} and CN^- (40 μM) in DMSO.

pH study:

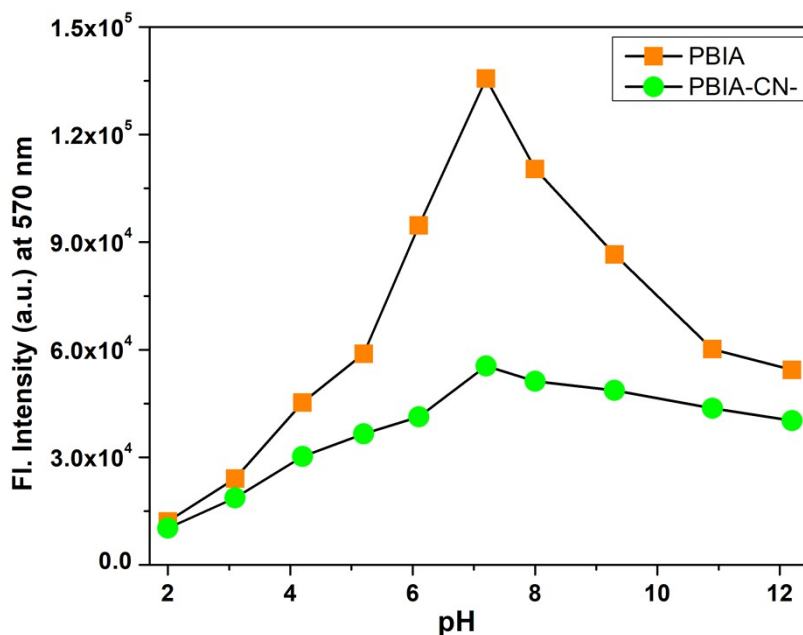


Fig. S12: pH study of PBIA for CN⁻ (from fluorescence spectra).

Effect of pH was also examined for absorption spectroscopy in case of PBIA and PBIA-CN⁻. For PBIA, we observed that the absorption spectra with lowering of pH value shows red shift with decrease in absorption value at 455 nm. Whereas for higher pH, the spectra appear with slight blue shift with increase in absorption value at 455 nm. The values were plotted against pH range of 2 to 12. In addition, for PBIA-CN⁻ in acidic condition, we observed that the absorption peak at 425 nm displays red shift with decrease in absorption value at 425 nm, whereas, in basic condition the absorption value shows slight increment. (Fig.S13).

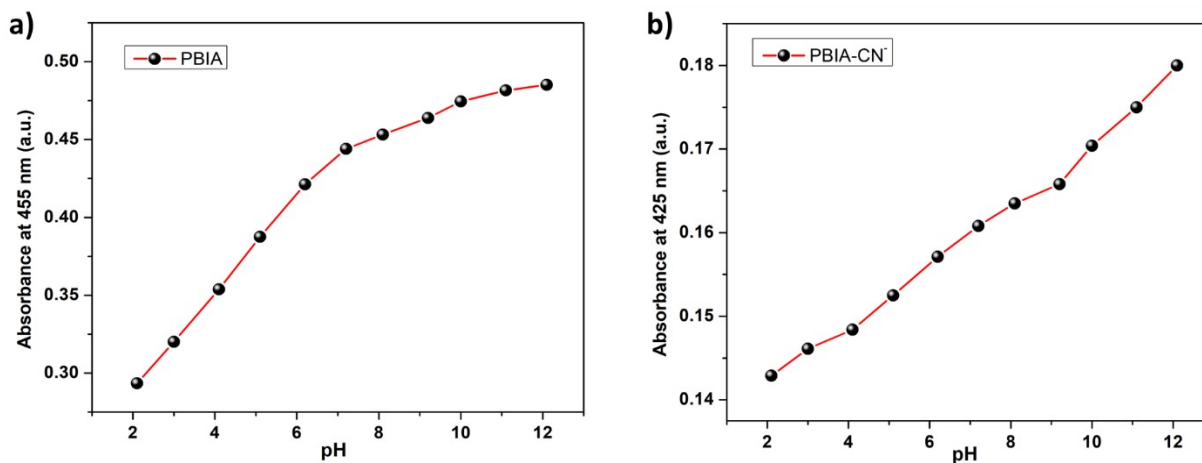


Fig. S13: pH study of PBIA (a) and for PBIA-CN⁻ (b) (from absorption spectra).

Stern-Volmer plot:

The fluorescence quenching is explained by the Stern–Volmer equation

$$F_0/F = 1 + K_{sv} [Q] \dots \dots \dots (1)$$

where F_0 and F are the fluorescence intensities in the absence and presence of CN^- , respectively. K_{sv} is the Stern–Volmer quenching constant and $[Q]$ is the concentration of the $[\text{CN}^-]$. The K_{sv} value is obtained with a slope from the plot of F_0/F versus $[Q]$ and found to be $1.16 \times 10^3 \text{ M}^{-1}$ respectively. The quenching constant value suggested a good interaction between the probe PBIa and CN^- .

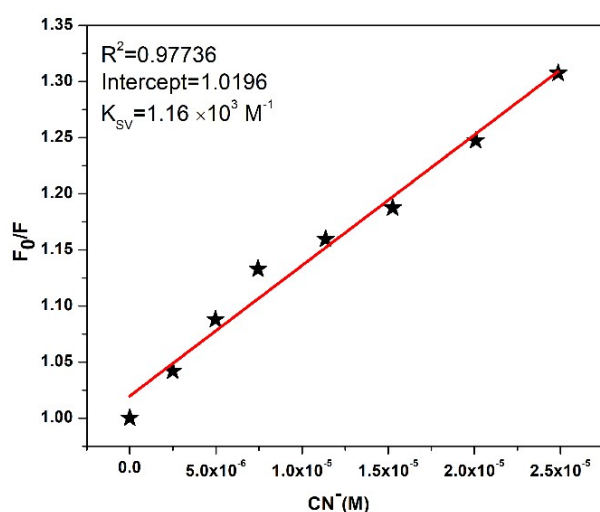


Fig. S14: Stern-Volmer plot for CN^- .

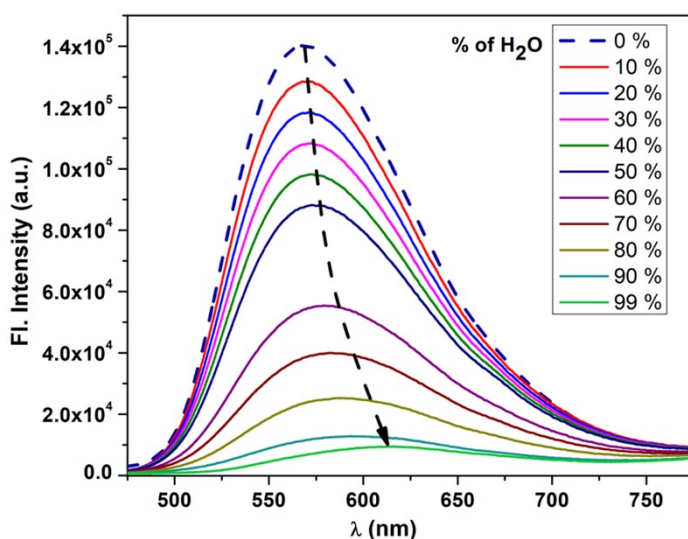


Fig. S15: Emission spectra of PBIa (20 μM) in DMSO with different water fractions (f_w) ($\lambda_{\text{ex}} = 430 \text{ nm}$).

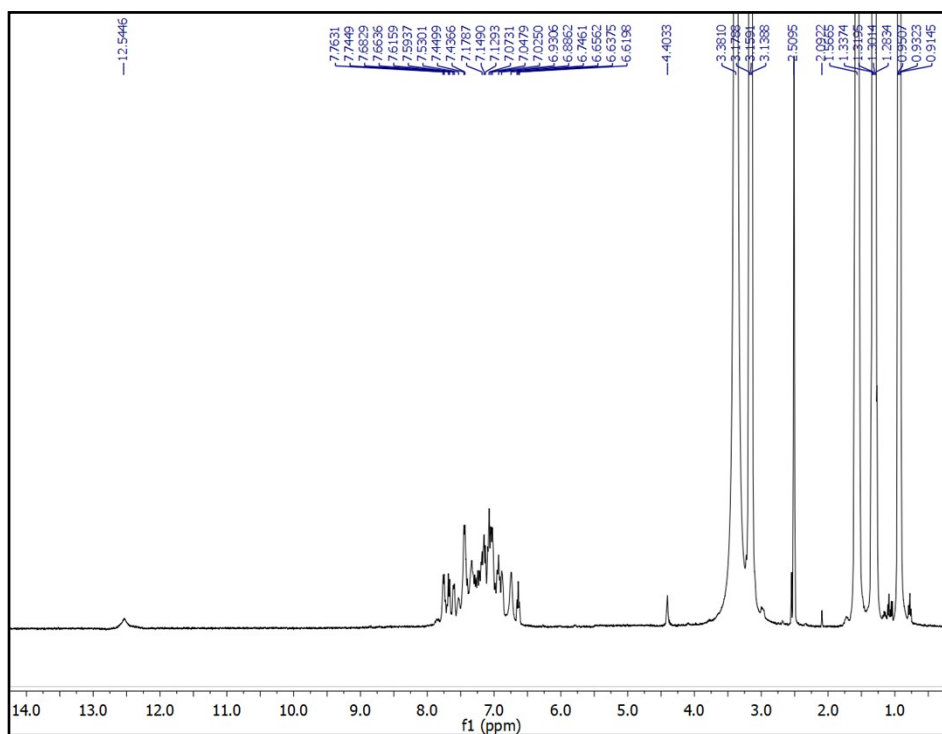


Fig. S16: ^1H NMR (400 MHz) spectra of the PBIA-CN adduct in DMSO-d_6

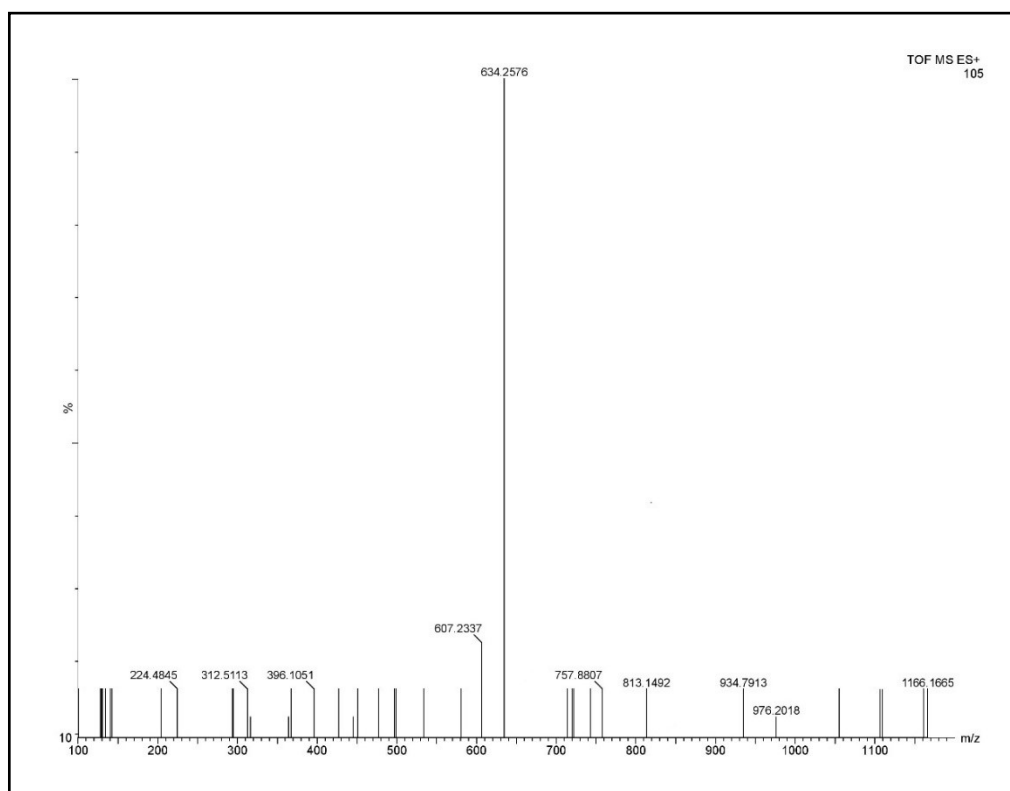


Fig. S17: HRMS of the PBIA-CN adduct.

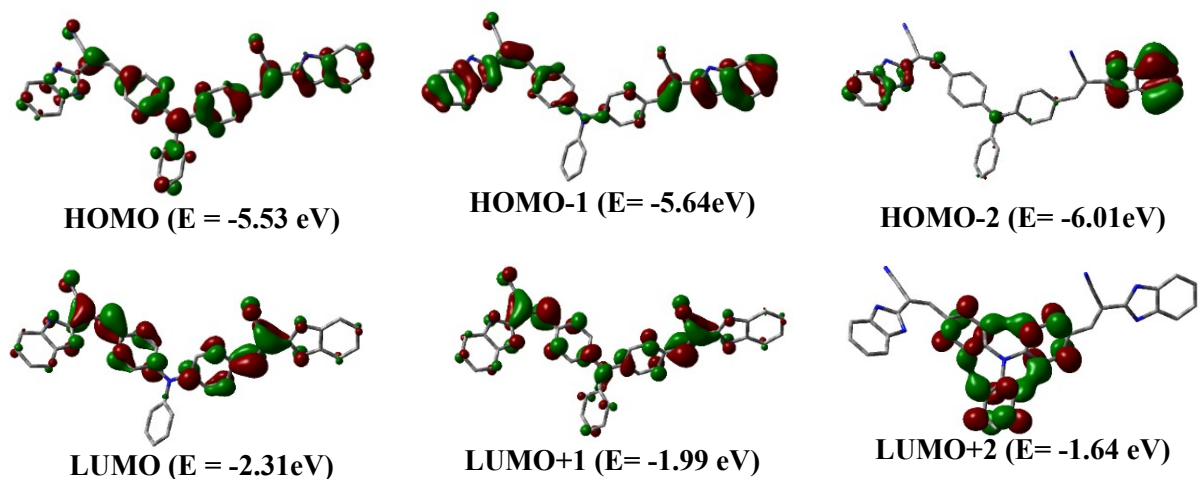


Fig. S18. Contour plots of some selected molecular orbitals of PBIA.

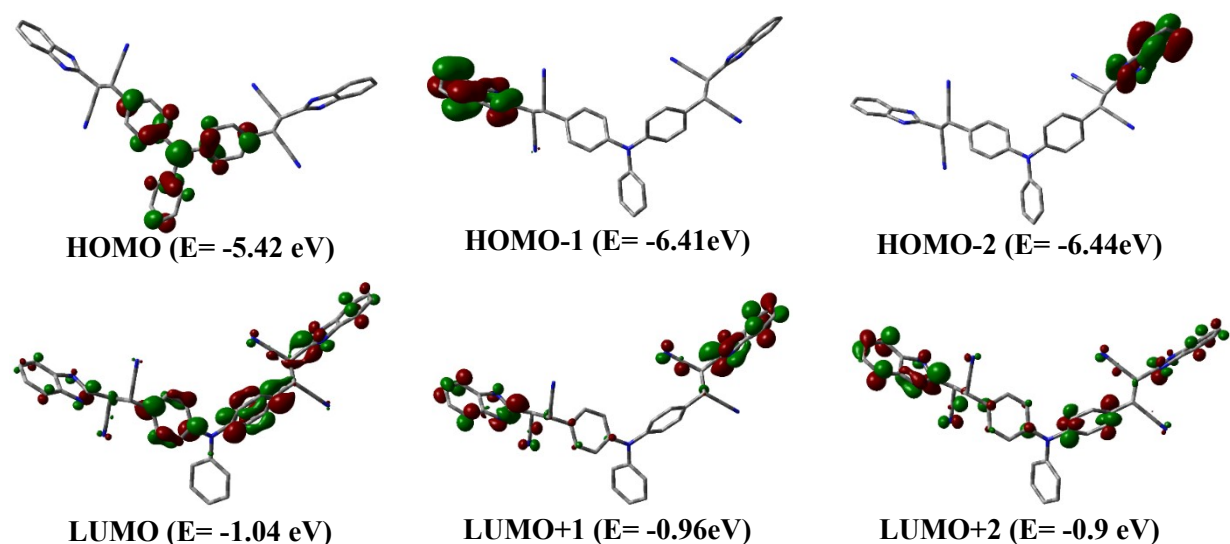


Fig. S19. Contour plots of some selected molecular orbitals of PBIA-CN⁻.

MTT assay:

The MTT assay demonstrates that PBIA imparts a negligible effect on cell viability at low doses but at higher doses, the viability of the cells was compromised. Cell viability represented in Fig.S13 indicates that from 1 to 200 μM concentration PBIA shows a high number of viable cells, which signifies that PBIA is safe to use in a biological system, although the cells have lower survivability in higher concentration. The IC_{50} was found

to be 179.727 μM and hence for subsequent experiments, the treatment dose was selected at 10 μM as the amount of dosage should be less than IC_{50} value.

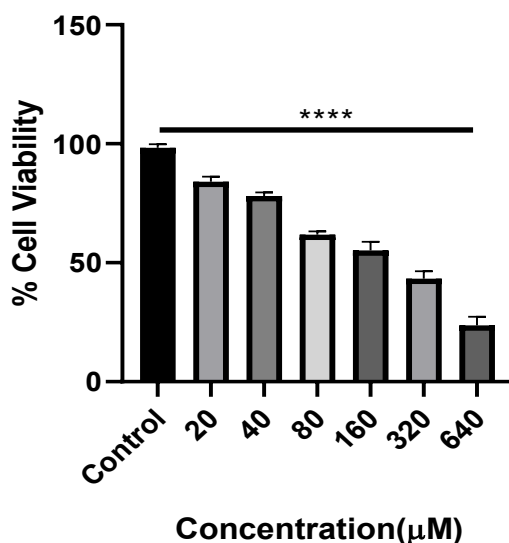


Fig. S20. Cell survivability of MDA-MB 231 cells exposed to different PBIA concentration. Data are representative of at least three independent experiments and bar graph shows mean \pm SD, **** $p < 0.0001$.

Application of PBIA in real water sample analysis:

The good selectivity and sensitivity towards cyanide makes our probe appropriate for real water sample analysis. Hence, to validate the reliability of PBIA to detect cyanide in real water samples, we collected water from Jadavpur University campus lake, tap and drinking water supplied to us. At first water samples were filtered through Whatman no. 1 filter paper to remove the suspended particles. Then blank experiment was conducted to check if there were any dissolved CN^- ions in water samples, but the results were negative as there were no change in probes colour under UV light.

Here our purpose was not to ascertain amount of CN^- in water, but to utilize the real water samples instead of deionized water to make CN^- solutions and conduct titration studies. Hence, cyanide salt was spiked in the stated water samples separately to prepare known concentration of cyanide solutions. Then fluorescence spectral studies were carried out using PBIA with addition of cyanide ion for quantitative measurement of CN^- ion in real water samples (Fig. S21, Fig. S22, Fig. S23). We observed almost similar spectroscopic response

with our previous controlled titration experiment (Fig. 2). Then standard calibration curves were constructed for determination of CN^- ion, which exhibited good linear relationship between the fluorescence of cyanide treated PBIA solution with cyanide concentration. The percentage of recovery were measured which was above 96 % (Table 1).

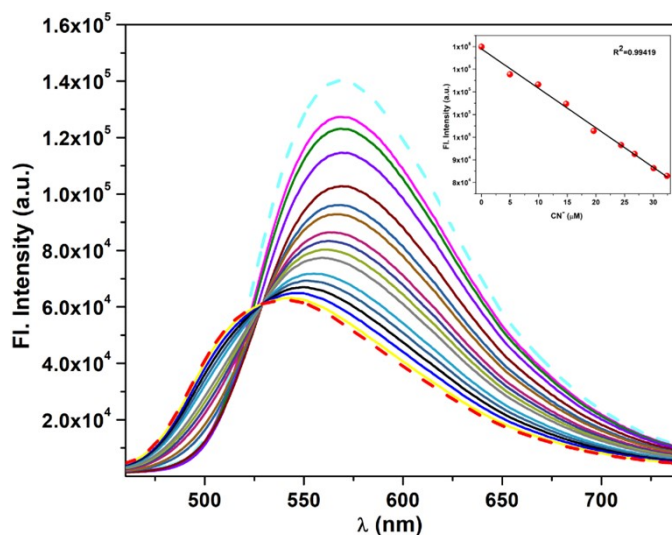


Fig. S21: Fluorescence spectral titration of the probe solution PBIA (20 μM , DMSO) with the addition of CN^- in drinking water. Inset: linear fitting plot of fluorescence of probe solution PBIA at 570 nm.

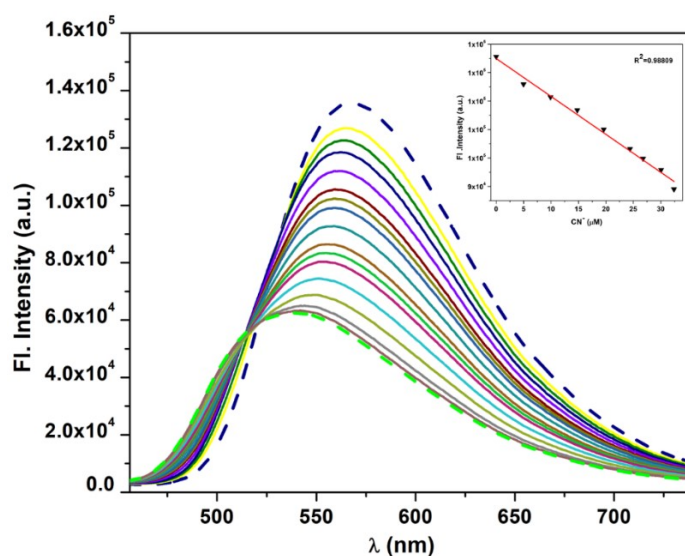


Fig. S22: Fluorescence spectral titration of the probe solution PBIA (20 μM , DMSO) with the addition of CN^- in tap water. Inset: linear fitting plot of fluorescence of probe solution PBIA at 570 nm.

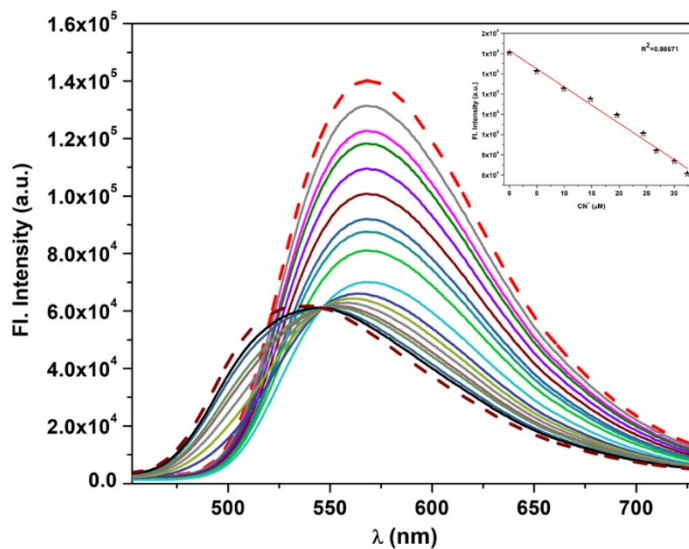


Fig. S23: Fluorescence spectral titration of the probe solution PBI A (20 μ M, DMSO) with the addition of CN^- in lake water. Inset: linear fitting plot of fluorescence of probe solution PBI A at 570 nm.

TableS1. Vertical electronic transitions of PBI A and PBI A- CN^- calculated by TDDFT/CPCM method

Compd.	λ (nm)	E (eV)	Osc. Strength (f)	Key excitations
PBI A	526.10	2.3567	1.6875	(99 %) HOMO \rightarrow LUMO
	439.11	2.8235	0.2083	(97 %) HOMO \rightarrow LUMO+1
	395.92	3.1315	0.1137	(96 %) HOMO-1 \rightarrow LUMO
	357.60	3.4671	0.2311	(89 %) HOMO-1 \rightarrow LUMO+1
	355.80	3.4846	0.1809	(72%) HOMO-4 \rightarrow LUMO
	289.05	4.2893	0.1095	(76 %) HOMO \rightarrow LUMO+3
PBI A-CN^-	343.60	3.6083	0.6200	(91%) HOMO \rightarrow LUMO
	327.03	3.7913	0.1126	(69%) HOMO \rightarrow LUMO+1
	314.21	3.9459	0.1191	(41%) HOMO \rightarrow LUMO+3
	303.82	4.0808	0.1315	(52%) HOMO \rightarrow LUMO+2
	301.94	4.1063	0.1047	(42%) HOMO \rightarrow LUMO+4

Determination of fluorescence Quantum Yields (Φ) of PBIA and its complex with CN^-

The luminescence quantum yield was determined using coumarin-153 as reference dye. The compounds and the reference dye were excited at the similar wavelength and the emission spectra were then studied. The area of the emission spectrum was integrated and the quantum yield is determined according to the following equation:

$$\phi_S/\phi_R = [A_S / A_R] \times [(Abs)_R / (Abs)_S] \times [n_S^2/n_R^2]$$

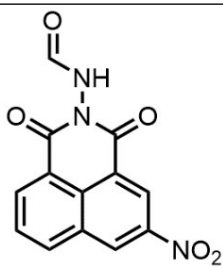
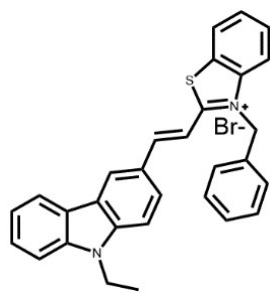
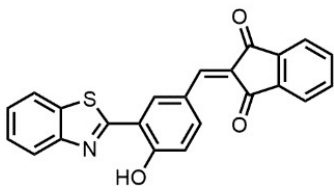
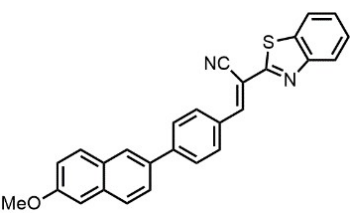
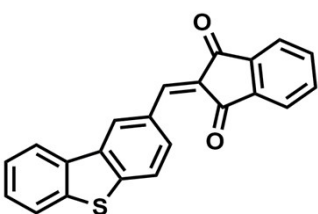
Here, ϕ_S and ϕ_R are the luminescence quantum yields of the sample and reference dye, respectively. A_S and A_R are the area under the emission spectra of the sample and the reference respectively, $(Abs)_S$ and $(Abs)_R$ are the respective optical densities of the sample and the reference solution at the wavelength of excitation, and n_S and n_R stand for the values of refractive index for the respective solvent used for the sample and reference.

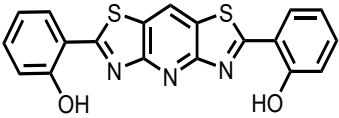
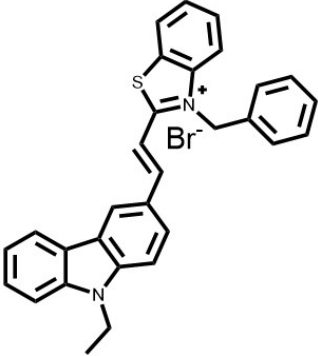
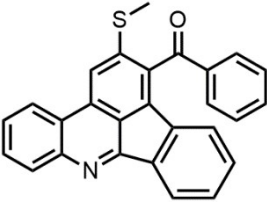
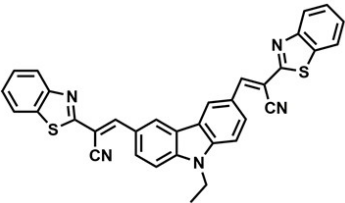
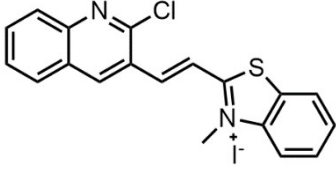
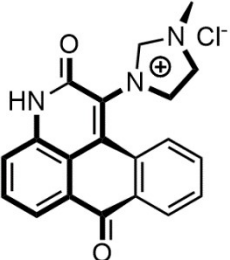
The quantum yields of PBIA and PBIA- CN^- are determined using the above mentioned equation and the values are found to be 0.148 and 0.074 respectively.

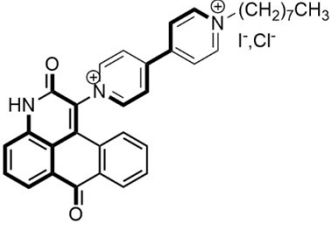
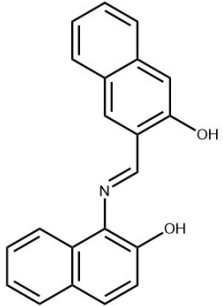
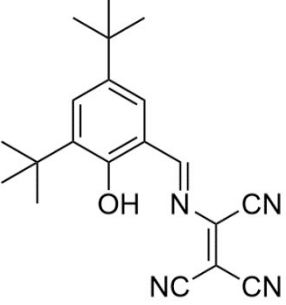
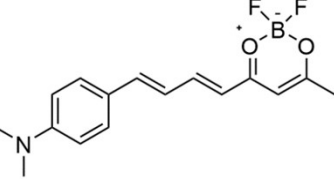
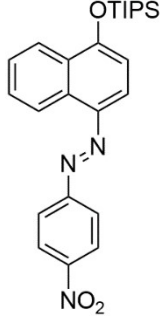
Table S2: Fluorescence lifetime data

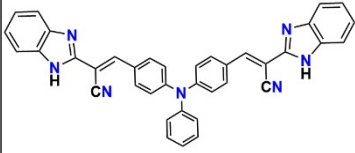
DMSO(Solvent)	Quantum yield(ϕ)	τ (ns)	$K_f(10^8 \times \text{S}^{-1})$	$K_{nr}(10^8 \times \text{S}^{-1})$
PBIA	0.148	0.50	2.95	17.02
PBIA-CN^-	0.074	1.99	0.37	4.63

Table S3: Sensor PBIAs towards CN^- compared to others previously reported receptors

Probe	Type	Solvent System	Detection limit	Reference
	$\text{CN}^-/\text{Fe}^{3+}$ and H_2S Turn-on and UV-absorption	5% aqueous DMSO	17.5 nM, 8.69 mM and 8.1 mM	<i>RSC Adv.</i> , 2020, 10 , 8751
	CN^- Ratiometric	DMSO/ H_2O (3: 2, v/v, pH = 7.4)	3.39×10^{-7}	<i>J. Mater. Chem. B.</i> , 2019, 7 , 4620
	CN^- Ratiometric	DMSO/ H_2O (7:3)	1.4×10^{-7} M	<i>RSC Adv.</i> , 2022, 12 , 8570
	CN^- Ratiometric	DMSO/ H_2O (10 mM HEPES buffer, 1: 1 v/v, pH 7.4	$2.1(\pm 0.0022) \times 10^{-8}$ M	<i>Anal. Methods.</i> , 2022, 14 , 3209
	CN^- Turn-off	DMSO/ H_2O (1:99, v/v)	2.26×10^{-7} M	<i>J. Photochem. Photobiol. A.</i> , 2021, 405 , 112993

	CN ⁻ Ratiometric	MeOH:H ₂ O (9 : 1).	75 nM	<i>New J. Chem.</i> , 2019, 43 , 13001
	CN ⁻ Ratiometric	DMSO/H ₂ O (3: 2, v/v, pH = 7.4).	3.39×10^{-7} M	<i>J. Mater. Chem. B</i> , 2019, 7 , 4620
	CN ⁻ Ratiometric	ACN/H ₂ O (9 : 1)	2.95×10^{-8} M	<i>Sens. Diagn.</i> , 2023, 2 , 337
	CN ⁻ Turn-on	DMSO-H ₂ O (4/1, v/v)	3.75 nM	<i>J. Lumin.</i> , 2018, 201 , 419-426
	CN ⁻ Turn-on	HEPES buffer/DMF (70 : 30 v/v)	—	<i>Anal. Methods</i> , 2018, 10 , 2368
	CN ⁻ Ratiometric	100% H ₂ O	0.13 pM	<i>Anal. Chim. Acta</i> , 2023, 1267 , 341376.

	<p>CN⁻ Turn-on</p>	<p>HEPES (pH 7.4): EtOH (1:1)</p>	<p>1 nM</p>	<p><i>Sens. Actuators B Chem.</i>, 2020, 304, 127396.</p>
	<p>CN⁻ Turn-on</p>	<p>DMF/H₂O (1:1, v/v)</p>	<p>0.21 μM</p>	<p><i>J. Photochem. Photobiol. A</i>, 2022, 424, 13651.</p>
	<p>CN⁻ Turn-on</p>	<p>H₂O:DMSO (1:1 v/v)</p>	<p>1.3 μM</p>	<p><i>Methods</i>, 2023, 215, 1-9.</p>
	<p>CN⁻ Turn-on</p>	<p>H₂O/THF (8/2, v/v)</p>	<p>2.23 μM</p>	<p><i>Spectrochim. Acta-A: Mol. Biomol. Spectrosc.</i>, 2022, 271, 20882.</p>
	<p>CN⁻, Colorimetric</p>	<p>ACN/ H₂O</p>	<p>2.73×10⁻⁶ mol L⁻¹</p>	<p><i>Spectrochim. Acta-A: Mol. Biomol. Spectrosc.</i>, 2021, 260, 119950.</p>

	CN ⁻ Ratiometric	DMSO	$(6.56 \pm 0.26) \times 10^{-8}$ (M)	This work
---	--------------------------------	------	--------------------------------------	-----------